AJNR Am J Neuroradiol 20:1259–1267, August 1999

Analysis of Cystic Intracranial Lesions Performed with Fluid-Attenuated Inversion Recovery MR Imaging

Italo Aprile, Francesca Iaiza, Antonino Lavaroni, Riccardo Budai, Pierluigi Dolso, Cathryn A. Scott, Carlo A. Beltrami, and Giuliano Fabris

***BACKGROUND AND PURPOSE*: T1-, T2-, and proton density (PD)-weighted sequences are used to characterize the content of cystic intracranial lesions. Fluid-attenuated inversion recovery (FLAIR) MR sequences produce T2-weighted images with water signal saturation. Therefore, we attempted to verify whether FLAIR, as compared with conventional techniques, improves the distinction between intracranial cysts with a free water-like content versus those filled with a non-free water-like substance and, consequently, aids in the identification of these lesions as either neoplastic/inflammatory or maldevelopmental/porencephalic.**

***METHODS*: Forty-five cystic intracranial lesions were studied using T1-weighted, T2-weighted, FLAIR, and PD-weighted sequences. By means of clustering analysis of the ratio in signal intensity between the cystic intracranial lesions and CSF, the intracranial lesions were classified as filled with a free water-like content or with a non-free water-like substance. The results were compared with their true content as evaluated either histologically or on the basis of clinical, neuroradiologic, and follow-up features (necrotic material, 13 cases; accumulation of intercellular proteinaceous/myxoid material, eight cases; keratin, five cases; CSF, 19 cases). Cystic intracranial lesions were divided into two clinical groups, neoplastic/inflammatory and maldevelopmental/porencephalic, to evaluate the level of accuracy of each MR technique. The difference in absolute value signal intensity between CSF and cystic intracranial lesion content was calculated on FLAIR and PD-weighted images.**

***RESULTS*: PD-weighted and FLAIR sequences, unlike T1- and T2-weighted sequences, accurately depicted all cystic intracranial lesions containing necrotic or myxoid/proteinaceous intercellular material (non-free water-like) and most CSF-containing cystic intracranial lesions (free water-like). All imaging techniques inaccurately showed some of the keratin-containing cystic intracranial lesions and pineal cysts. The overall error rate was 22% for T1-weighted, 27% for T2-weighted, 9% for FLAIR, and 13% for PD-weighted sequences. The signal intensity difference between CSF and cystic intracranial lesion content was higher with FLAIR imaging.**

***CONCLUSIONS*: FLAIR imaging depicts far more accurately the content of cystic intracranial lesions and better reveals the distinction between maldevelopmental/porencephalic and neoplastic/inflammatory lesions than do conventional sequences. FLAIR has the added advantage of a higher signal intensity difference between cystic intracranial lesions and CSF.**

Many intracranial lesions have cystic features on MR images. The cystic appearance arises from an abrupt transition between tissues with different physicochemical properties and corresponds histologically to a wide spectrum of diseases. Cystic intracranial lesions may correspond either to true cysts (lined by epithelial, ependymal, or meningothelial cells), porencephalic pseudocysts (all containing CSF), dermoid and epidermoid cysts (containing keratin), the appearance of which on MR images may simulate CSF, or may correspond to pseudocystic neoplastic or inflammatory lesions because of the accumulation either of necrotic or of intercellular myxoid or proteinaceous material (1, 2). From a clinical point of view, it is important

Received February 20, 1998; accepted after revision, March 23, 1999.

From the Departments of Neuroradiology (I.A., F.I., A.L., P.D., G.F.) and Neurology-Clinical Neurophysiology (R.B.), S. Maria della Misericordia General Hospital, and the Institute of Pathology (C.A.S., C.A.B.), University of Udine, Udine, Italy.

Address reprint requests to Italo Aprile, MD, Department of Neuroradiology, S. Maria della Misericordia General Hospital, via G. Pieri, 33100 Udine, Italy.

TABLE 1: Diagnosis of cystic intracranial lesions

Diagnosis	No.	Surgery	Cystic Content
Neoplastic/Inflammatory CILs			
Glioblastoma	6	+	Necrotic material
Metastasis from carcinoma	6	+	Necrotic material
Abscess	1	+	Necrotic material
Microcystic meningioma	1	+	Intercellular material
Astrocytoma	2	+	Intercellular material
Pleomorphic xantoastrocytoma	1	+	Intercellular material
Hemangioblastoma	1	+	Intercellular material
Schwannoma, recurrence	1	+	Intercellular material
Oligodendroglioma, recurrence	1	+	Intercellular material
Pilocytic astrocytoma, recurrence	1	+	Intercellular material
Maldevelopmental/Porencephalic CILs			
Dermoid cyst	1	+	Keratin debris
Epidermoid cysts	4	+ (2)*	Keratin debris
Porencephalic pseudocyst	5	−	…
Glioependymal cyst	5	−	…
Arachnoid cyst	4	−	…
Choroidal fissure cyst	2	−	…
Pineal cyst	3	−	…

Note.—The clinical group and diagnoses of the cystic intracranial lesions (CILs) are shown together with the features of the cystic content as seen histologically. All cases submitted to surgery were examined histologically. The intercellular material observed was either proteinaceous, myxoid or edematous. * Only 2 of the 4 epidermoid cysts were evaluated histologically.

to be able to distinguish between those cystic intracranial lesions that require surgery and those that do not, because the former represent a potentially life-threatening condition for the patient (neoplastic or inflammatory) whereas the latter (maldevelopmental or porencephalic) usually require only follow-up.

The study of the features of the content of these cystic intracranial lesions by means of traditional MR techniques (T1-weighted, T2-weighted, and PD-weighted imaging) contributes to their identification (1, 2) and therefore helps in planning further therapeutic decisions. Fluid-attenuated inversion recovery (FLAIR) sequences are T2-weighted images in which the free water signal is saturated; therefore, free water has a low signal whereas other tissues with a long T2-weighted relaxation time have a higher signal (3). Considering that the content of cystic intracranial lesions may be similar to CSF or to a tissue rich in lipids or proteinaceous material, FLAIR sequences ought to be able to delineate readily the difference between these lesions because of their contrasting physicochemical characteristics.

The aim of this study was twofold. First, we sought to evaluate the accuracy of the FLAIR technique in comparison with T1-, T2-, and PD-weighted sequences for identifying the type of content of cystic intracranial lesions classified as free, water-like or non-free water-like. Second, we attempted to verify the ability of the four techniques to illustrate correctly the nature of cystic intracranial lesions as maldevelopmental or porencephalic on the one hand and neoplastic or inflammatory on the other. The nature of cystic intracranial lesions was verified by means of either histologic analysis or clinical and neuroradiologic features and follow-up (4).

Methods

Using MR imaging, forty-five consecutive patients (23 women, 22 men; age range, 20−83 years; mean age, 49.5 years) with cystic intracranial lesions were studied.

MR Techniques

All of the examinations were performed using a 1-T system with 15-mT/m gradients. T2- and PD-weighted (fast spin-echo: 4000/90, 22/1 [TR/first-echo TE, second-echo TE/excitations] matrix, 250 × 256, echo train, 5), T1-weighted (spin echo: 570/15/2; matrix, 256 × 256), and fast-FLAIR (7000/150/1; inversion time, 2200; matrix, 250 × 256) images were acquired. The imaging time of fast-FLAIR pulse sequences was adjusted to saturate free water. The sections were 5 mm in thickness in the same plane of orientation; for each pulse sequence, the plane chosen for evaluation was that which was best fitted to visualize the lesion. T1-weighted images after intravenous contrast medium administration (0.1 mmol/kg) were acquired in 24 cases.

The ratio between the cystic content and the CSF signal intensity on T1-weighted, T2-weighted, PD-weighted, and FLAIR images was calculated using the following formulas:

$$\text{R-T1} = (\text{SI T1 lesion} - \text{SI T1 CSF}) \div \text{SI T1 CSF} \times 100$$

$$\text{R-T2} = (\text{SI T2 lesion} - \text{SI T2 CSF}) \div \text{SI T2 CSF} \times 100$$

$$\text{R-PD} = (\text{SI PD lesion} - \text{SI PD CSF}) \div \text{SI PD CSF} \times 100$$

$$\text{R-FLAIR} = (\text{SI FLAIR lesion} - \text{SI FLAIR CSF}) \div \text{SI FLAIR CSF} \times 100$$

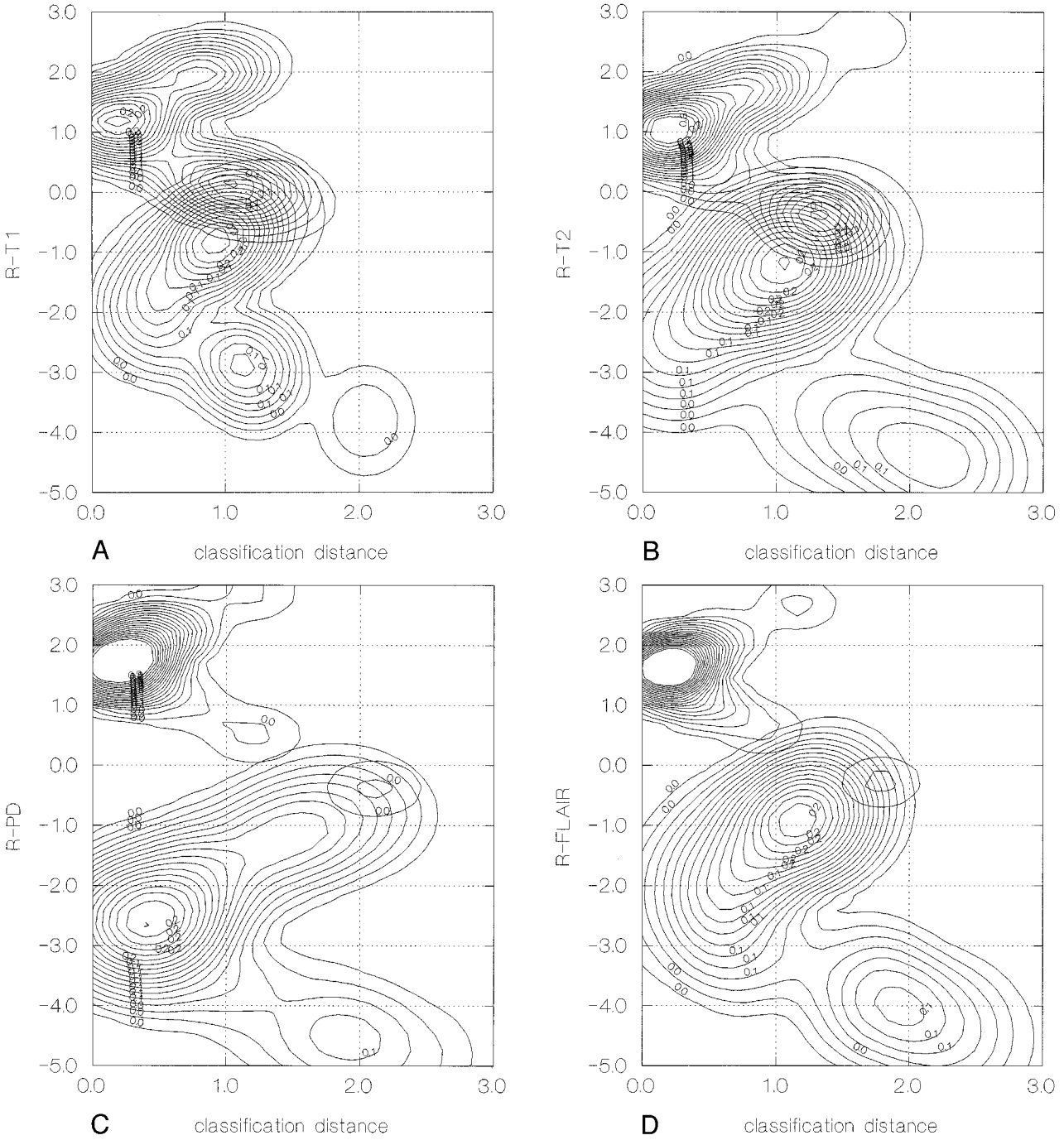

FIG 1. Graphic representation of the probability distribution of cystic intracranial lesions being clustered around the center of two groups: free water-like and non-free water-like–filled lesions. The *x* axis indicates the distance of each case from the center of each of the two groups. The *y* axis represents the contrast resolution between CSF and cystic intracranial lesion content. The *z* axis represents the probability of being clustered in one of the two groups. As the distance from the center of one of the two clusters increases, the probability coefficient decreases.

A, Calculated on T1-weighted images (R-T1).
B, Calculated on T2-weighted images (R-T2).
C, Calculated on PD-weighted images (R-PD).
D, Calculated on FLAIR images (R-FLAIR).

SI represents the signal intensity, which was calculated at a specific workstation by means of regions of interest located in the same areas of the images obtained with all sequences. For each cystic intracranial lesion, the arithmetical average of values of signal intensity was calculated and the data were normalized using a logarithmic function. The values obtained represent the contrast resolution between the content of the cystic intracranial lesion and CSF.

On PD-weighted and FLAIR images, another ratio was calculated to obtain the difference in signal intensity between cystic intracranial lesion content and CSF by using the following formulas:

TABLE 2: Classification of CILs

Diagnosis	Cystic Content	R-T1		R-T2		R-PD		R-FLAIR	
		NFWL	FWL	NFWL	FWL	NFWL	FWL	NFWL	FWL
Neoplastic/inflammatory CILS									
Glioblastoma	Necrotic material	6	0	5	1	6	0	6	0
Metastasis from carcinoma	Necrotic material	5	1	6	0	6	0	6	0
Abscess	Necrotic material	1	0	1	0	1	0	1	0
Microcystic meningioma	Intercellular material	1	0	1	0	1	0	1	0
Astrocytoma	Intercellular material	1	1	2	0	2	0	2	0
Pleomorphic xantoastrocytoma	Intercellular material	1	0	1	0	1	0	1	0
Hemangioblastoma	Intercellular material	1	0	1	0	1	0	1	0
Schwannoma, recurrence	Intercellular material	1	0	1	0	1	0	1	0
Oligodendroglioma, recurrence	Intercellular material	1	0	1	0	1	0	1	0
Pilocytic astrocytoma, recurrence	Intercellular material	1	0	1	0	1	0	1	0
Maldevelopmental/Porencephalic CILS									
Dermoid cyst	Keratin debris	0	1	1	0	1	0	1	0
Epidermoid cysts	Keratin debris	2	2	3	1	3	1	1	3
Porencephalic pseudocyst	CSF	1	4	4	1	0	5	0	5
Glioependymal cyst	CSF	2	3	0	5	0	5	0	5
Arachnoid cyst	CSF	0	4	1	3	0	4	0	4
Choroidal fissure cyst	CSF	0	2	0	2	0	2	0	2
Pineal cyst	CSF	3	0	2	1	2	1	2	1

Note.—Classification of the cystic intracranial lesions (CILs) on the basis of R-T1, R-T2, R-PD and R-FLAIR values (see text) as non free water-like (NFWL) and free water-like (FWL) in relation to clinical grouping, diagnosis and nature of cystic content.

$$\text{R1-PD} = (\text{SI PD lesion} - \text{SI PD CSF}) \div (\text{SI PD lesion} + \text{SI PD CSF})$$

$$\text{R1-FLAIR} = (\text{SI FLAIR lesion} - \text{SI FLAIR CSF}) \div (\text{SI FLAIR lesion} + \text{SI FLAIR CSF})$$

Histologic Analysis

Histologic examinations were conducted in 23 cases. Samples from the lesions were fixed in buffered formalin and embedded in paraffin. Hematoxylin and eosin slides were examined, and, when necessary, immunocytochemical stains were performed with anticytokeratin CAM 5.2, antiglial fibrillary acidic protein, and antiprotein S-100 antibodies.

Classification of Cystic Intracranial Lesions

Table 1 shows the histologic, or clinical and neuroradiologic diagnosis, or both, of the cystic intracranial lesions considered in this study and their membership in one of the two clinical groups: neoplastic/inflammatory or maldevelopmental/porencephalic. The nature of the cystic content of all cases that were evaluated histologically is also shown.

In the 22 cases for which no histologic sample was available, the lesions were mostly incidental findings, and no surgical treatment was recommended. Their nature was inferred on the basis of morphologic features, postcontrast behavior, medical history, and clinical outcome, which remained unchanged during a follow-up period of at least 6 months (4). The five patients with porencephalic pseudocysts had previous histories of surgical resection for primary brain tumors (two glioblastomas, two anaplastic astrocytomas, and one medulloblastoma). Two of the four cases classified as epidermoid cysts were not submitted to surgery. The cases studied after contrast medium administration included all neoplastic/inflammatory cystic intracranial lesions and one epidermoid, one glioependymal, and one pineal cyst.

Statistical Analysis

Clustering analysis (k-means) was performed separately on R-T1, R-T2, R-PD, and R-FLAIR values to divide the cases into statistically different groups (5). *P* values were considered significant when equal to or below .05. The difference in signal intensity between PD-weighted and FLAIR images was calculated using the Student's *t* test, considering that the distribution of R1-PD and R1-FLAIR values was normal using the Lilliefors test ($P > .05$).

Results

Clustering analysis was able to depict two significantly ($P < .0001$) different groups of lesions on the basis of R-T1, R-T2, R-PD, and R-FLAIR values (Fig 1). The first group, regardless of the type of sequence used, was composed of cystic intracranial lesions with a content signal intensity pattern different from that of free water (non-free water-like); the second group was composed of cystic lesions with a content signal intensity pattern similar to that of free water (free water-like). Using clustering analysis, no further subdivision of each of the two groups resulted in significant *P* values.

Table 2 shows the classification of cystic intracranial lesions contents as free water-like and non-free water-like by using the four sequences in relation to their definite diagnosis and in relation to the division of cystic intracranial lesions into the two clinical groups: neoplastic/inflammatory and maldevelopmental/porencephalic. When compared with their true content, the classification of cystic intracranial lesions into free water-like or non-free water-like consistently led to correct diagnosis when using FLAIR and PD-weighted sequences for

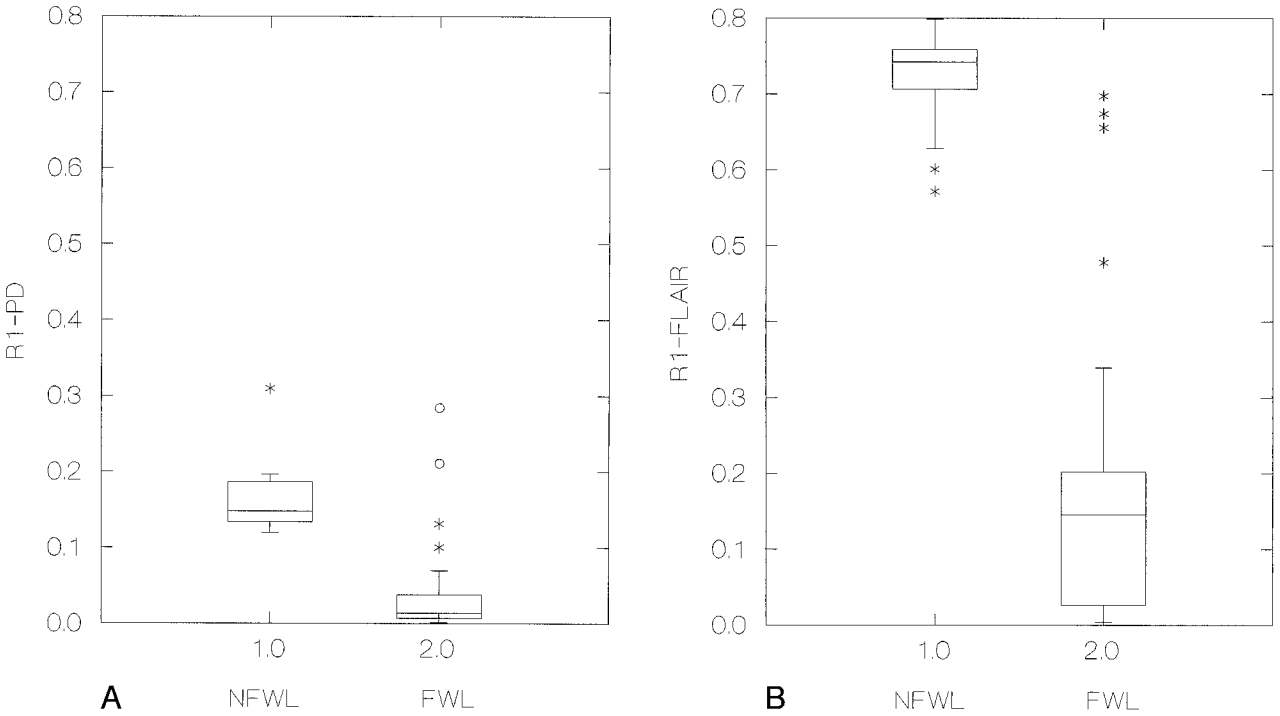

FIG 2. Distribution of the ratio in signal intensity difference between content of cystic inracranial lesions and CSF using the Box-Jenkins method on the two groups of lesions: free water-like and non-free water-like.

A, PD-weighted sequences.

B, FLAIR sequences.

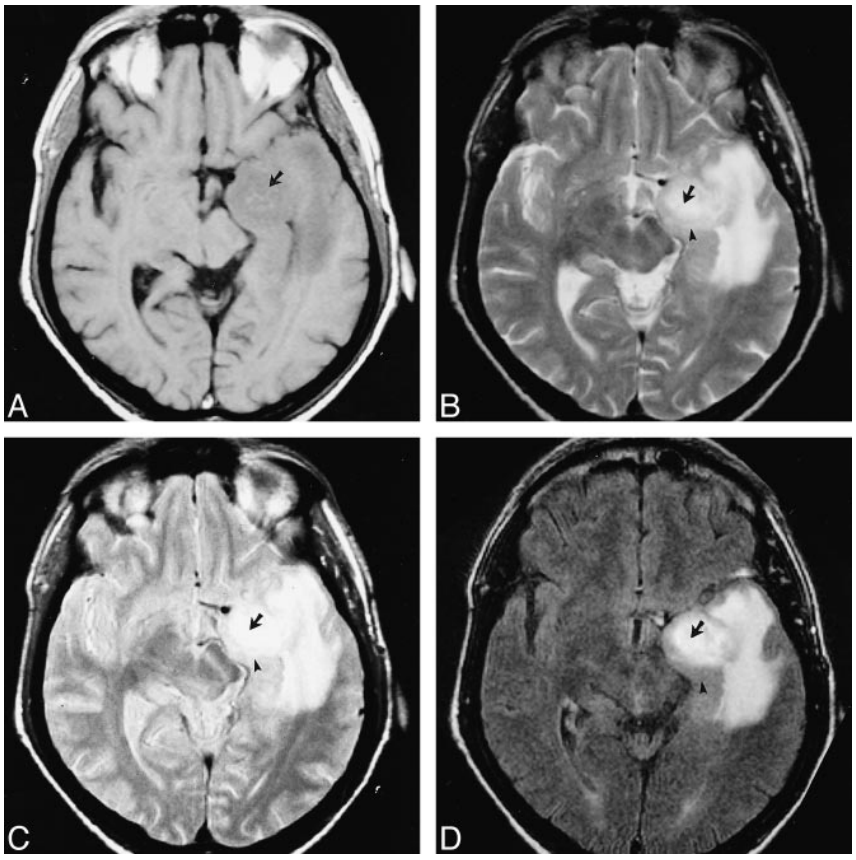

FIG 3. Left temporal glioblastoma.

A, T1-weighted sequence. The tumor has a central part (*arrow*) with a dyshomogeneous but mostly hyperintense signal in comparison with cysternal and ventricular CSF.

B, T2-weighted image. The solid part of the tumor (*arrowhead*) is hypointense, and the necrotic part (*arrow*) and perilesional edema are hyperintense, similar to CSF. The region of interest was taken from the central, necrotic part (*arrow*) in all the images.

C, PD-weighted image. Necrosis (*arrow*) is easily distinguished from the solid neoplastic tissue (*arrowhead*) but with less resolution than that achieved using the T2-weighted image. The necrotic area appears slightly hyperintense in comparison with CSF.

D, FLAIR sequence. Both the necrotic tissue (*arrow*) and perilesional edema remain hyperintense. The tumor tissue (*arrowhead*) remains hypointense and the necrotic material (*arrow*) is highly hyperintense, whereas CSF has a low signal.

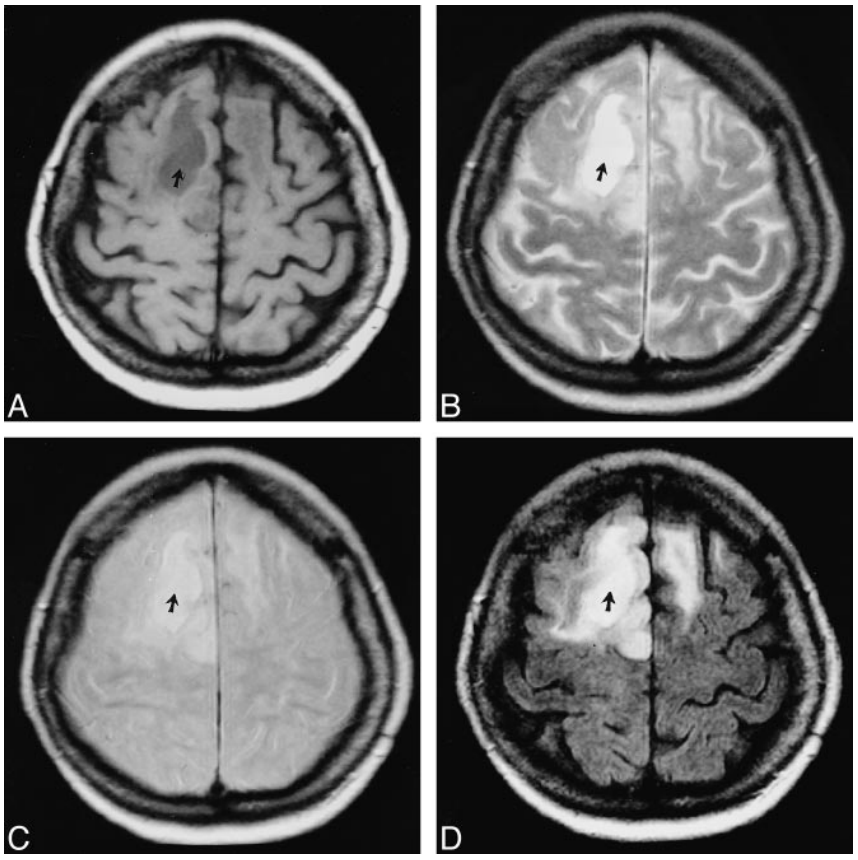

FIG. 4. Right frontal recurrence of an oligodendroglioma. The difference in signal intensity between CSF and cystic content is probably attributable to protein debris, typical of neoplastic lesions. This feature is evident on all sequences but is more obvious with the FLAIR sequence. With this pulse sequence, both the neoplastic tissue and peritumoral edema are appreciated more easily considering the saturation of the CSF signal in the sulci.

A, T1-weighted image. The cystic content (*arrow*) is slightly hyperintense in comparison with CSF (in the cortical sulci).

B, T2-weighted image. The neoplastic cystic content (*arrow*) has an elevated signal intensity in comparison with CSF.

C, PD-weighted image. The cystic content signal intensity is slightly hyperintense (*arrow*) in comparison with CSF.

D, FLAIR pulse sequence. The cystic content (*arrow*) shows an elevated signal intensity.

the imaging of the necrotic lesions or of those with accumulation of intercellular material. T1- and T2-weighted sequences, however, led to one diagnostic error each in the imaging of necrotic cystic intracranial lesions and the T1-weighted sequence led to one diagnostic error in the imaging of cystic intracranial lesions with accumulation of intercellular material (Table 2).

All sequences inaccurately depicted the keratin content of dermoid and epidermoid cysts and the CSF content of pineal cysts. The CSF content of porencephalic pseudocysts also was not evident in one and four cases on T1- and T2-weighted images. Furthermore, T1-weighted findings led to the misclassification of two glioependymal cysts as being non-free water-like and T2-weighted findings led to the misclassification of one arachnoid cyst as being non-free water-like (Table 2).

When compared with clinical grouping, all sequences led to some classification errors. These errors were 22% (10 of 45 cases) for T1-weighted, 27% (12 of 45 cases) for T2-weighted, 9% (4 of 45 cases) for FLAIR, and 13% (6 of 45 cases) for PD-weighted sequences.

T1- and T2-weighted sequences led to the misclassification of two and one cystic intracranial lesion, respectively, in the neoplastic/inflammatory group, whereas FLAIR and PD-weighted sequences led to the correct classification for all lesions. Most errors occurred in the maldevelopmental/porencephalic clinical group: eight (33%) of 24 cases with T1-weighted, 11 (46%) of 24 cases with T2-weighted, four (17%) of 24 cases with FLAIR, and six (25%) of 24 cases with PD-weighted sequences.

The signal intensity difference between CSF and cystic content on FLAIR images, when compared with PD-weighted images, resulted in a highly significant P value ($<.00001$) (Fig 2). Figures 3 through 7 show examples of a glioblastoma, a recurrence of an oligodendroglioma, an arachnoid cyst, a choroidal fissure cyst, and an epidermoid cyst, as seen with T1-weighted, T2-weighted, FLAIR, and PD-weighted sequences.

Discussion

The content of cystic intracranial lesions may be similar to CSF or may be rich in lipids or proteinaceous material; conventional T2-weighted sequences are unable to delineate these two types of cystic lesions because their relaxation times and, hence, their signal intensities are very similar. On the other hand, with PD-weighted sequences, the signal depends on the spin density of the cystic content; therefore, this technique is the most suitable for discriminating between these two types of cysts and is considered reliable for this purpose (1, 2).

In this study, the identification of the content of cystic intracranial lesions containing necrotic material was accurate in all cases using PD-weighted and FLAIR imaging, with one misclassification each using T1- and T2-weighted sequences alone.

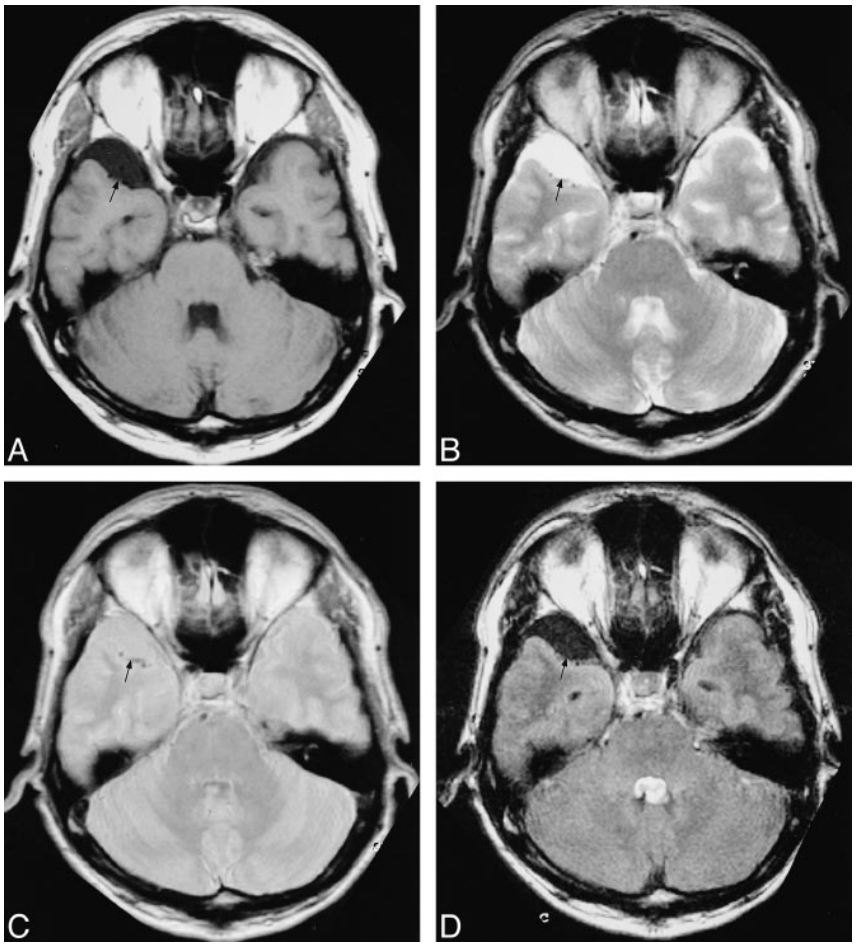

FIG 5. Right temporal arachnoid cyst. The cyst's content (*arrow*) is isointense to CSF (see controlateral cortical cysterns, fourth ventricle, lateral ventricles) in all of the sequences. This appearance is attributable to the similarity of CSF and cystic content.

A, T1-weighted sequence.

B, T2-weighted sequence.

C, PD-weighted sequence.

D, FLAIR sequence. On the FLAIR image, the hyperintensity seen in the fourth ventricle is owing to flow artifact.

This high level of correct classification occurred because both coagulative and lytic necrosis generate material rich in lipids and proteins (6), which is easily distinguishable from free water with all sequences (Fig 3) (1, 2).

Cystic intracranial lesions with accumulation of intercellular material included five untreated primary brain tumors and three recurrences. Some of these tumors appear cystic because, characteristically, they show accumulation of proteinaceous or myxoid material, the physicochemical properties of which determine, in most MR sequences, a non-free water-like image. Tumor recurrences, regardless of histologic features, show edematous areas frequently associated with dilated blood vessels and evidence of previous hemorrhages that lead to the non-free water-like MR findings (1, 2, 6−8). Here again, only one error was made using the T1-weighted sequence because of the marked difference in composition between the intercellular material and CSF. T2-weighted, FLAIR, and PD-weighted sequences all led to the correct identification of these lesions as having non-free water-like material (Fig 4).

On both PD-weighted and FLAIR images, the content of porencephalic pseudocysts, arachnoid, glioependymal, and choroidal fissure cysts appeared free water-like because of their equivalence to CSF (Fig 5 and 6) (9−13); however, T1- and T2-weighted sequences led to a certain number of errors (three and five, respectively). All sequences were inaccurate in depicting the content of two types of lesions: pineal cysts and dermoid and epidermoid cysts. Some pineal cysts not only were classified inaccurately but also revealed a nonhomogeneous signal intensity. This phenomenon is possibly attributable to the relatively frequent histologic observation of foci of hemorrhage or hemorrhagic debris within these lesions (6, 14) and may justify the images of cysts with non-free water-like contents even though T1-weighted sequences did not reveal hyperintensity, owing to metahemoglobin, in any of these cases. It is possible that even small quantities of hematic debris may determine a non-free water-like appearance of these cysts (6, 14−17).

The keratin content of dermoid and epidermoid cysts was identified as free water-like in a few cases regardless of the sequence used, even though non-CSF material is present within these lesions. The MR behavior of the content of these cysts depends on the amount of lipids present; for example, on T1-weighted sequences, if the presence of lipids is low, the content appears similar to CSF, whereas if it is high, its signal is clearly different from that of CSF (18−22). The varied results observed with the

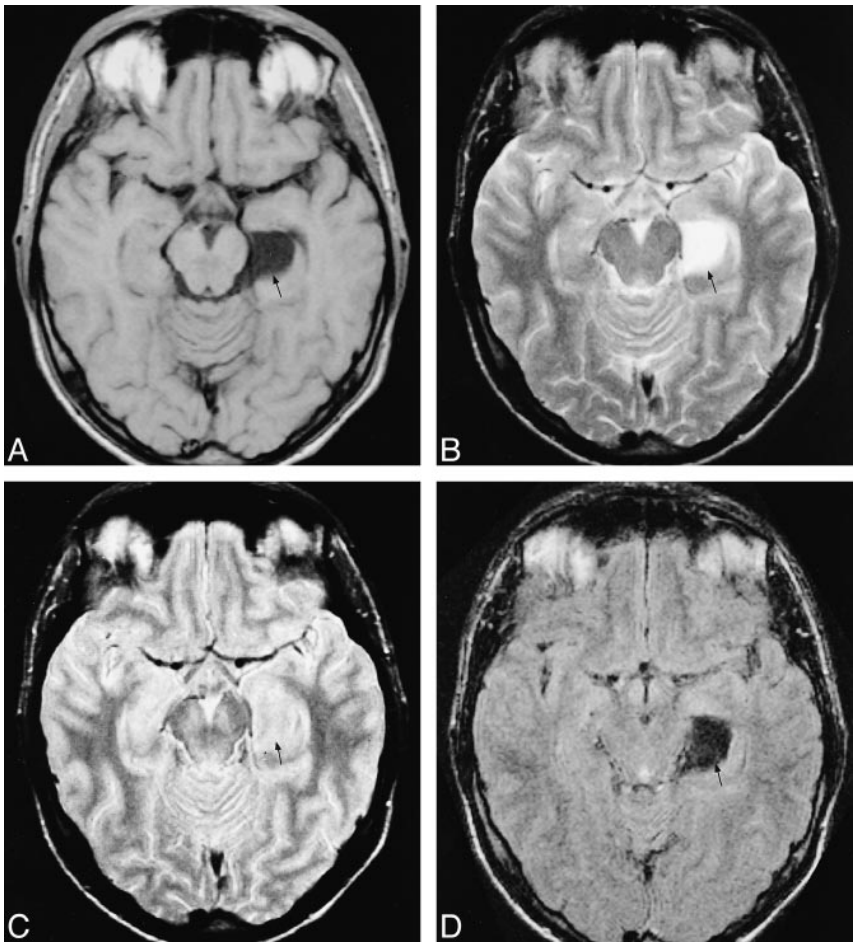

FIG 6. Left temporal choroidal fissure cyst. The cystic content (*arrow*) is very similar to CSF, and, for this reason, its signal intensity is equivalent to CSF (see interpedunclar and other cisterns) in all of the sequences.

A, T1-weighted sequence.

B, T2-weighted sequence.

C, PD-weighted sequence. On the PD-weighted image, the lesion is not clearly evident because its content is isointense to the temporal cortex.

D, FLAIR sequence.

sequences used in this study are clearly related to the variability in lipid content of this type of cystic intracranial lesion (Fig 7). In any case, the expected appearance on MR images of keratin-containing cystic intracranial lesions is CSF-like (6, 14); accordingly, T1-weighted and FLAIR sequences led to fewer misclassifications than did T2- and PD-weighted sequences.

From a clinical point of view, cystic intracranial lesions were divided into two groups: neoplastic/inflammatory and maldevelopmental/porencephalic. The first group of cystic intracranial lesions, considering the characteristics of their content, were expected to produce a non-free water-like image, and the second were expected to produce a free water-like signal.

The results of this study, therefore, confirm previous findings presented in the literature (1, 2) regarding the high level of accuracy of the PD-weighted technique in delineating the clinical grouping of cystic intracranial lesions when compared with T1- and T2-weighted sequences. Furthermore, the results show that FLAIR imaging is as precise as PD-weighted imaging in accurately illustrating all of the neoplastic/inflammatory cystic intracranial lesions examined and that FLAIR imaging led to fewer diagnostic errors than did PD-weighted imaging when analyzing maldevelopmental/porencephalic cystic intracranial lesions. Hence, FLAIR sequences may be used as an alternative to PD-weighted sequences in the evaluation of cystic intracranial lesions.

A further advantage was found in using FLAIR over PD-weighted sequences in the examination of cystic intracranial lesions. Even though the ratios of R1-FLAIR and R1-PD–weighted imaging were the same for any one lesion classified either as free, water-like or non-free water-like, the absolute value of the difference of the signal between the content of the cystic intracranial lesion and CSF was much higher using FLAIR imaging. The result was that visual inspection was sufficient to diagnose any lesion as containing CSF or non-CSF material without having to calculate signal intensity on regions of interest.

Conclusion

Considering the clinical importance of distinguishing cystic intracranial lesions that require further therapy from those that need only follow-up, the FLAIR technique may be used confidently as an alternative to PD-weighted imaging in the evaluation of cystic intracranial lesions. Furthermore, apart from showing fewer artifacts, such as blurring and edge enhancement typical of PD-weighted im-

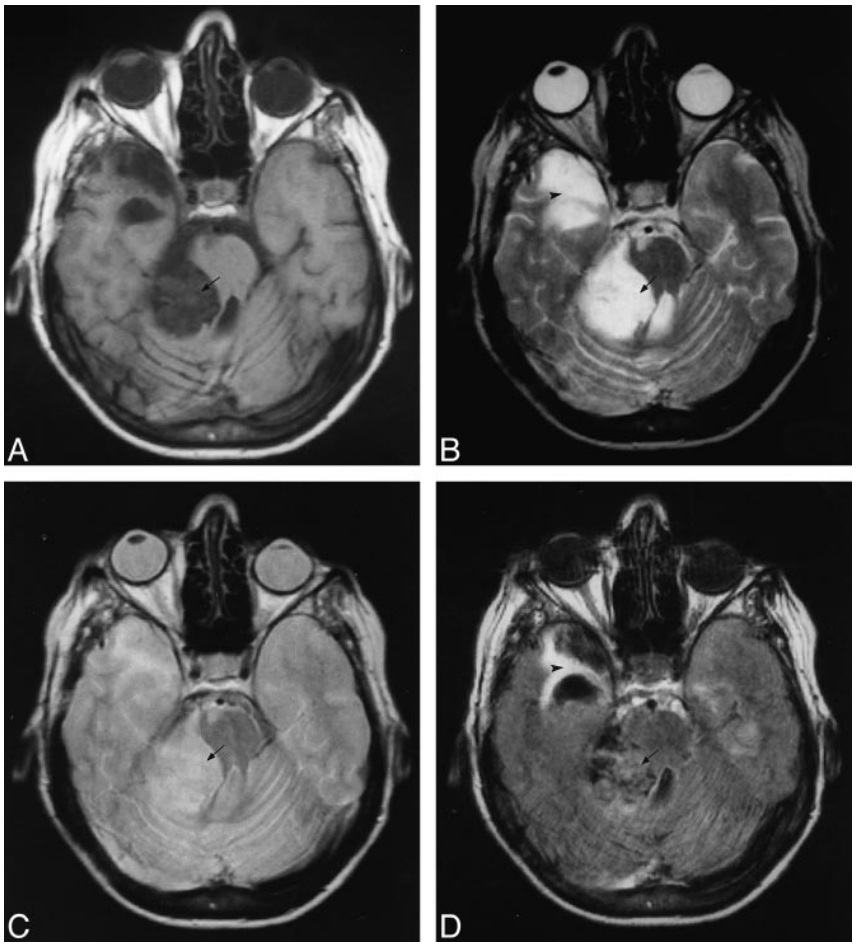

FIG 7. Right pontocerebellar cistern epidermoid cyst.

A, T1-weighted image. The cystic content (*arrow*) is slightly hyperintense to CSF (see compressed fourth ventricle).

B, T2-weighted image. The cystic content (*arrow*) is isointense to CSF. The T2-weighted image also shows a right temporal gliotic area (*arrowhead*).

C, PD-weighted sequence. The cystic content (*arrow*) is slightly hyperintense to CSF.

D, FLAIR sequence. The cystic content (*arrow*) is markedly hyperintense when compared with CSF. In this case, the content of the cyst was not saturated from using FLAIR and the lesion was misclassified as non-free water–like. The FLAIR image also shows a right temporal gliotic area (*arrowhead*).

ages acquired with the fast spin-echo technique (23), FLAIR sequences have the added advantage of a far better resolution capable of differentiating between non-free water-like cystic intracranial lesions and CSF.

References

1. Kjos BO, Brant-Zawadzki M, Kucharczyc W, Kelly WM, Norman D, Newton TH. **Cystic intracranial lesions. Magnetic resonance imaging.** *Radiology* 1985;155:363–369
2. Go KG, Hew JM, Kamman RL, Molenaar WM, Pruim J, Blaauw EH. **Cystic lesion of the brain. A classification based on pathogenesis with consideration of histological and radiological features.** *Eur J Radiol* 1993;17:69–84
3. Tsuchiya K, Mizutani Y, Hachiya J. **Preliminary evaluation of fluid-attenuated inversion-recovery MR in the diagnosis of intracranial tumors.** *AJNR Am J Neuroradiol* 1996;17:1081–1086
4. Chang KH, Song IC, Kim SH, et al. **In vivo single-voxel proton MR spectroscopy in intracranial cystic masses.** *AJNR Am J Neuroradiol* 1998;19:401–405
5. Hartigan JA, Wong MA. **A K-means clustering algorithm. Algorithm AS 136.** *Appl Stat* 1979;28:126–130
6. Burger PC, Scheithauer BW. **Tumors of the Central Nervous System.** Washington: Armed Forces Institute of Pathology; 1994; 1–435
7. Wasenko JJ, Hochhauser L, Stopa EG, Winfield JA. **Cystic meningiomas. MR characteristics and surgical correlations.** *AJNR Am J Neuroradiol* 1994;15:1959–1965
8. Zee CS, Chen T, Hinton DR, Tan M, Segall HD, Apuzzo ML. **Magnetic resonance imaging of cystic meningiomas and its surgical implications.** *Neurosurgery* 1995;36:482–488
9. Penning L. **Cerebrospinal fluid (CSF) ex vacuo.** *Radiol Clin (Basel)* 1976;45:425–434
10. Wiener SN, Pearlstein AE, Eiber A. **MR imaging of intracranial arachnoid cysts.** *J Comput Assist Tomogr* 1987;11:236–241
11. Heier LA, Zimmerman RD, Amster JL, Gandy SE, Deck MD. **Magnetic resonance imaging of arachnoid cysts.** *Clin Imaging* 1989;13:281–291
12. Ismail A, Tampieri D, Melanson D, Pokrupa R, Villemure JG, Bertrand G. **Glioependymal cysts. CT and MR findings.** *J Comput Assist Tomogr* 1992;16:860–864
13. Sherman JL, Camponovo E, Citrin CM. **MR imaging of CSF-like choroidal fissure and parenchymal cysts of the brain.** *AJNR Am J Neuroradiol* 1990;11:939–945
14. McLendon RE, Tien RD. **Tumors and tumor-like lesions of maldevelopmental origin.** In: Bigner DD, McLendon RE, Bruner JM, eds. *Russel and Rubinstein's Pathology of Tumors of the Nervous System.* 6th ed. London: Arnold; 1998;295–370
15. Lee DH, Norman D, Newton TH. **MR imaging of pineal cysts.** *J Comput Assist Tomogr* 1987;11:586–590
16. Fetell MR, Bruce JN, Burke AM, et al. **Non-neoplastic pineal cysts.** *Neurology* 1991;41:1034–1040
17. Sandhu JS, McLaughlin JR, Gomez CR. **Characteristics of incidental pineal cysts on magnetic resonance imaging.** *Neurosurgery* 1989;25:636–639
18. Lunardi P, Missori P. **Supratentorial dermoid cysts.** *J Neurosurg* 1991;75:262–266
19. Netsky MG. **Epidermoid tumors. Review of the literature.** *Surg Neurol* 1988;29:477–483
20. Steffey DJ, De Filipp GJ, Spera T, Gabrielsen TO. **MR Imaging of primary epidermoid tumors.** *J Comput Assist Tomogr* 1988; 12:438–440
21. Tampieri D, Melanson D, Ethier R. **MR imaging of epidermoid cysts.** *AJNR Am J Neuroradiol* 1987;10:351–356
22. Vion-Dury J, Vincentelli F, Jiddane M, et al. **MR imaging of epidermoid cysts.** *Neuroradiology* 1987;29:333–338
23. Tien RD, Felsberg GJ, MacFall J. **Practical choices of fast spin echo pulse sequence parameters. Clinically useful proton density and T2-weighted contrast.** *Neuroradiology* 1992;35:38–41